Full-Scale Demonstration of Higher Harmonic Control for Noise and Vibration Reduction on the XV-15 Rotor

Khanh Nguyen, Mark Betzina, Cahit Kitaplioglu
Army/NASA Rotorcraft Division
NASA Ames Research Center
Moffett Field, CA

Abstract

A higher harmonic control (HHC) investigation was conducted on a full-scale, isolated XV-15 Rotor in helicopter mode in the NASA Ames 80- by 120-Foot Wind Tunnel to independently control noise, vibration, and trim. The higher harmonic blade root pitch was generated using swashplate oscillations. The radiated blade-vortex interaction (BVI) noise footprint was measured on a plane beneath the rotor with eight microphones mounted on an acoustic traverse. Test results showed that HHC is highly effective in reducing BVI noise, achieving a 12 dB reduction in peak noise level within the noise footprint. Blade pressure feedback was demonstrated to be a viable method for closed-loop noise control. Perturbations in trim parameters and test conditions had small to moderate effects on noise reduction with HHC. Some noise reduction was achieved with no increase in vibratory hub loads. Increases in control loads due to HHC generally limited further noise reduction. The vibration controller achieved about 50 percent reduction in vibratory hub loads with control loads limiting the HHC amplitude. An automatic trim controller was demonstrated to be robust, reaching all target thrust and flapping schedules under all conditions tested.

Introduction

Tiltrotor aircraft, employing swiveling rotors that allow the aircraft to take-off and land like helicopters but also fly like propeller airplanes, have great potential to relieve airport congestion. Tiltrotor aircraft have been proposed to ferry passengers directly to and from vertiports located near urban areas and mass transit. However, such a proposal has been hampered by concerns over the noise levels generated by these aircraft during landing approach [1]. Furthermore, tiltrotors operated in edgewise flight can generate higher vibration levels than helicopters due to the stiff-inplane blades [2]. The development of low-noise, low-vibration tiltrotors is essential in the successful implementation of this revolutionary mode of air transportation and greatly expands the utility of tiltrotor aircraft.

During landing approach, as a rotor descends into its own wake, large pressure fluctuations are generated on the rotor blade surfaces as each blade interacts with the vortices generated previously from the blade tips. The parallel blade-vortex interactions (BVI) are the source of the distinctly impulsive noise radiated from rotor blades. Tiltrotors can generate significantly higher noise than helicopters due to higher blade loading. Blade vortex interaction noise is a community disturbance that severely restricts civilian operations of rotorcraft in populated areas and is a source of early detection in military operations [3].

While passive noise reduction methods can reduce BVI noise, they can impose severe penalties on the aircraft performance, the aircraft empty weight, or the rotor structural loads. Classical passive methods for noise reduction employ rotor solidity (blade chord or blade number) to reduce blade loading, blade tip shape to reduce tip vortex strength, or reduced rotor tip speed [4]. Recently, wind tunnel tests of the ERATO model rotor with a non-traditional blade planform has demonstrated significant noise reduction, up to 7 dB compared to a more traditional reference rotor in equivalent BVI conditions [5]. Besides the noise benefits, the ERATO rotor exhibited better rotor performance than the reference rotor but had some setbacks due to blade structural loads.

The development of low-noise approach profiles has shown potential for noise reduction of tiltrotor aircraft. By exploiting the nacelle-tilt capability and wing-flap configuration, several approach profiles flight-tested on the XV-15 aircraft have shown up to 7 dB in noise reduction [6] compared to a baseline profile. Operational methods offer an additional benefit since they

Presented at the American Helicopter Society 56th Annual Forum, Virginia Beach, VA, May 2-4, 2000.

can be used along with low-noise rotor designs to yield larger noise reduction.

In addition to passive methods and approach operations, methods using active blade pitch also have potential to reduce rotorcraft noise. In particular, higher harmonic control (HHC) was shown to be effective in reducing BVI noise on helicopters. In this method, the swashplate was excited with dynamic actuators at the blade-number (N) harmonic, resulting in blade pitch oscillations at N–1, N, and N+1 per-rev (P) in the rotating frame. Up to 6 dB in BVI noise reductions were reported independently by Brooks [7] and Splettstoesser [8] on two different model rotors using HHC. In both cases, noise reduction was accompanied by increases in vibratory hub loads. These test results led to the formation of the Higher-harmonic Aeroacoustic Rotor Test (HART), a multi-national cooperative research program aimed at exploring the physics of noise and vibration reduction with HHC. The HART has been conducted on a BO-105 model rotor in the DNW wind tunnel [9]. In addition to the wind tunnel tests, HHC benefits were also demonstrated in flight on a research Gazelle helicopter, achieving 3.5 EPNdB (Effective Perceived Noise) in BVI noise reduction [10].

Besides noise control, HHC has been conceived as an active control method for helicopter vibration. The HHC input generates the higher harmonic airloads to suppress the oscillatory blade loads that cause airframe vibration. Compared to current passive vibration control devices, HHC offers many benefits including better performance, weight savings, and robustness to changes in flight conditions. Results from both flight [11-13] and wind tunnel tests [14,15] demonstrated that HHC was very effective in suppressing helicopter vibration. A recent wind tunnel test of a semispan V-22 scaled model showed that HHC was also successful in reducing tiltrotor-induced vibration in the airplane mode [16].

Individual-blade-control (IBC) is another active control method that has shown potential to reduce both noise and vibration on helicopters. In this method, the pitch-links were replaced with high-frequency actuators that directly generated the active blade root pitch. Unlike HHC, an IBC system can generate any waveform within the bandwidth limit of the actuators. The IBC test of a full-scale four-bladed BO-105 rotor in the 40- by 80-Foot Wind Tunnel showed noise reduction of about 10 dB along with significant vibration reduction using a combination of 2P and 5P blade pitch harmonics [17]. Note that an HHC system using swashplate oscillation can not generate a 2P input while maintaining a four-bladed rotor in-track. Attempts to duplicate these wind tunnel results during a flight test of the BO-105 helicopter equipped with an IBC system showed noise reduction of more than 5 dBA [18]. Restricted control authority during the flight test, for safety-of-flight concerns, probably limited noise reduction with the IBC system.

Beside the blade root actuation methods using either HHC or IBC, blade-mounted control devices have also shown potential to reduce BVI noise. The test of a model rotor equipped with an active trailing-edge flap in the NASA Langley 14- by 22-Foot Subsonic Tunnel showed BVI noise reduction of more than 4 dB [19]. The flap schedule for such noise reduction was non-harmonic, being active only for a short azimuth range in the BVI region.

In an effort to develop low-noise low-vibration tiltrotors, an experiment was conducted at NASA Ames Research Center to evaluate several technologies on a full-scale XV-15 rotor in the 80- by 120-Foot Wind Tunnel. The HHC investigation described in this paper is a component of the Short Haul Civil Tiltrotor Program, which is an element of the Aviation System Capacity Program. The objectives were to independently reduce BVI noise and rotor vibratory hub loads and to automatically trim the rotor. Additional objectives of the test program were to acquire baseline acoustic data at different flight and operating conditions for both three- and four-bladed rotor configurations, and the results are presented in detail in Ref. 20. Besides noise and vibration control, an automatic trim controller was developed and tested during the wind tunnel entry. This trim study represents an important first step in the development of an automatic rotor control system for wind tunnel operations. The initial goal was to determine whether an automatic controller could perform rotor trim instead of manual operations.

Both open-loop and closed-loop results for noise reduction are presented in the paper. Specific findings with regard to HHC effectiveness at different flight conditions and the effects of trim perturbations and control amplitudes on noise reduction are presented. Secondary effects of HHC on the rotor structural loads, vibratory hub loads, and rotor performance are also included. In addition, the performance of the vibration and trim controllers is presented.

Test Description

Hardware Description. The installation of the XV-15 rotor in the 80- by 120-Foot Wind Tunnel, along with the microphone traverse in the foreground, is shown in Fig. 1. The right-handed rotor of the XV-15 aircraft was mounted on the NASA/Army Rotor Test Apparatus (RTA). The XV-15 rotor is a stiff-inplane hingeless rotor and has a gimballed hub connected to the RTA mast by a constant velocity joint. Test-specific

hardware, such as the swashplate, pitch-links, and hub adaptor, were built to allow attachment of the XV-15 rotor to the RTA. Designed as a compromise between the three- and four-bladed hub configurations, the swashplate provided a pitch-link arrangement that generated a 36 deg of flap up/pitch up coupling (negative δ_3) for the three-blade hub. This δ_3 value is different from that of the XV-15 aircraft, which is –15 deg. Table 1 lists the general rotor properties.

The RTA is a special-purpose test stand for rotor testing and includes an electric-drive motor, right-angle transmission, six-component balance, and both primary and dynamic control systems. The RTA was mounted on a three-strut support system, placing the rotor hub approximately 31 feet (1.24 rotor diameters) above the tunnel floor. The balance measured both steady and vibratory rotor hub loads, including the rotor thrust, drag (H-force), side force, pitching and rolling moments, and shaft torque. For this test, the rotor balance was not calibrated dynamically. The primary control system provided collective and cyclic input to trim the rotor.

Swashplate Excitations. The RTA dynamic control system consisted of three rotary hydraulic actuators located at 0, 180, and 270 deg azimuth under the swashplate to provide either steady or 3P excitations. The dynamic control system was locked-out when not in use. Steady input from the dynamic control system produced blade collective and cyclic pitch for trim control, while 3P excitations produced blade pitch harmonics at 2P, 3P, and 4P for noise and vibration control. Both types of input were superimposed with the trim input from the primary control system. The maximum HHC amplitude was nominally 2 deg. However, this magnitude was not reached during the wind tunnel test due to control system load limits under HHC excitation.

Instrumentation. Blade and control system strain gauges were installed at the critical load paths for safety-of-flight monitoring. A bar chart display of structural loads was monitored throughout the test to safeguard against fatigue damage to the rotor system and the RTA. Wind tunnel operations restricted oscillatory loads within the fatigue levels to ensure infinite life of structural components. These operating limits were maintained throughout the test.

Four pairs of dynamic (absolute) pressure transducers were mounted at blade radial stations of 0.65, 0.78, 0.85, and 0.95. The Kulite pressure transducers were surface-mounted at 5 percent chord from the leading edge, on both upper and lower surfaces at each radial location. The pressure transducer locations were chosen to capture the BVI events and utilized as feedback signals for noise control.

The gimbal was instrumented to provide blade flapping angle for trim. A blade pitch transducer, mounted across the pitch bearing, provided a direct measurement of the trim and HHC input. The rotor balance provided both rotor performance and dynamically-uncalibrated vibratory hub load measurements.

The BVI noise footprint was measured with an acoustic traverse consisted of eight microphones and was placed 1.8 rotor radii below the advancing side of the rotor disk. Relative to the rotor hub, the traverse microphones spanned 0.36 to 1.69 blade radii in the cross-flow direction and traversed from 0.2 to 2.0 blade radii in the streamwise direction. Figure 2 shows the microphone locations in the test section.

Wind Tunnel Data Acquisition. The wind tunnel data acquisition system has a low-speed and a high-speed chassis. The low-speed chassis acquired rotor performance, loads, and blade response data at 64 per-rev for 64 revolutions. The low-speed data were low-pass filtered at 100 Hz before being digitized by the data acquisition system.

High-speed data were limited to microphone and blade pressure signals. These data were low-pass filtered at 4 kHz and sampled at 2048 per-rev for 64 revolutions. The blade-vortex-interaction sound pressure level (BVI-SPL), a measure of BVI noise, was computed by summing all frequency bands from the 10^{th} to the 50^{th} blade passage harmonics (approximately 300 to 1500 Hz). This frequency range was selected to highlight the acoustic pulse, the main feature of the BVI event. Besides, the selection prevented the contamination of noise measurements due to reflections at the lower frequencies and background noise at both low and high frequencies [21]. The wind tunnel test section has a sound-absorbing liner that absorbs more than 90 percent of sound with frequencies higher than 250 Hz. In addition to the liner, sound-absorbing foam was attached to portions of the RTA and selected hard points in the test section to reduce local reflections.

HHC Controller. The HHC Controller provided an independent platform for data acquisition, control law execution, and controller output for both open-loop and closed-loop operations. The controller hardware consisted of a Windows-NT PC with a 266 MHz Pentium II processor, a 12-bit, 16 channel National Instruments (NI) AT-MIO-16E-1 data acquisition board, and a 12-bit, 6 channel NI AT-AO-10 board for data output. Dedicated HHC operations were developed in-house using Labview. During HHC operations, harmonics of the blade pitch input, instead of swashplate motions, were prescribed at the controller front panel. The controller automatically converted the input harmonics into a swashplate schedule in the collective, longitudinal and lateral cyclic modes. A conversion

matrix, pre-computed based on a least-squares method, transformed the blade pitch harmonics to harmonics of swashplate motion. Waveforms of swashplate motion were then generated and continuously fed to the output-board to drive the dynamic actuators.

HHC Control Algorithm. The control algorithm was based on the T-matrix approach, a harmonic control method, for the control of noise, vibration, and trim. The HHC plant model was

$$z_n = z_{n-1} + T_n(\theta_n - \theta_{n-1}) \quad (1)$$

where z_n was the controlled vector (or scalar), T_n was the T-matrix, θ_n was the vector of blade pitch harmonics, and n denoted the controller cycle. Depending on the control objectives, each element of the T-matrix represented the sensitivity of a controlled parameter to each harmonic of the blade pitch and was computed using a least-squares method with open-loop data. The controller update cycle was once per rotor revolution. With the plant model, the control law was formulated as an optimization problem:

$$\min (z_n^T Q z_n + \theta_n^T R \theta_n) \quad (2)$$

where Q and R were diagonal matrices assigning relative weightings to z_n and θ_n, respectively. The optimal control, including a relaxation factor r ($0 < r < 1$), was:

$$\theta_n = \theta_{n-1} + (1-r)\, C_n z_{n-1} \quad (3)$$

where

$$C_n = -(T_n^T Q T_n + R)^{-1} T_n^T Q \quad (4)$$

The relaxation factor r was introduced to reduce the controller update rate and allow smoothing of output waveforms during controller updates.

Feedback Parameters. Different feedback signals were used depending on the controlled parameters. For noise control, both microphone and blade pressure feedback were used independently. The feedback signals were computed in real time during closed-loop operations. For microphone feedback, selected microphone signals (maximum of four) were sampled at 512 per-rev over four revolutions. The Labview Fast-Fourier-Transform (FFT) routine was employed to compute the spectrum of the microphone signals. The equivalent BVI-SPL, used in the controller, consisted of 10^{th} to 50^{th} blade passage harmonics.

For the noise controller using blade pressure feedback, the controller aimed to reduce a measure of the pressure signals, pre-processed externally before being fed into the controller. The pressure signals were first bandpass-filtered to highlight the BVI events and then fed into the RMS meters to provide a measure of BVI energy. The RMS meter outputs were essentially constants for a test condition. The controller used the rms-pressure signals, sampled at 128 per-rev over four revolutions, as the feedback for noise control.

For vibration, the controller used signals from the rotor hub loads – thrust, H-force, side forces, and pitching and rolling moments. The 3P hub load components were extracted from the signals using a Labview FFT routine. The objective of the controller was to suppress the vibration index, a weighted-measure of the root-mean-square of the 3P hub load harmonics.

The automatic trim controller used the steady rotor thrust and the gimbal cyclic flapping as feedback parameters. For this controller, the goal was to minimize the difference between the target and the feedback trim values. For both vibration and trim control, the data were sampled at 128 per-rev over four revolutions.

Test Conditions. The test conditions for HHC investigation are shown in Table 2. A test condition was set to advance ratio μ, rotor loading C_T/σ, and shaft tilt α (positive values for rearward tilt). Unless specified otherwise, zero one-per-rev flapping was maintained during the test conditions. Therefore, the equivalent tip-path-plane angle of attack, based on gimbal flapping angle, was equal to the shaft tilt angle. Since the tip Mach number was known to have a major effect on the noise level, it was strictly maintained at 0.691 at all noise-related test conditions.

Results and Discussion

Control of BVI Noise

The effects of HHC on BVI noise were evaluated at four simulated landing approach conditions of the XV-15 tiltrotor aircraft as shown in Table 2. The maximum BVI noise condition in the table is the first condition listed: 0.17 advance ratio, 0.09 C_T/σ, and 3 deg rearward shaft tilt.

Open-loop Phase Sweeps. Open-loop phase sweeps using individual 2P–4P components of blade pitch were initially performed to explore the behavior of BVI noise under HHC excitation. These preliminary results were also used to assess vibratory hub loads and rotor structural loads during HHC application and allowed an evaluation of the signal processing techniques of blade pressure for closed-loop operations. The HHC amplitude was selected to remain uniform throughout the phase sweep while maintaining the structural loads within the operating limits. The BVI noise was measured with the microphone traverse parked at a location slightly ahead of the rotor disc. The BVI-Sound Pressure Level (BVI-SPL) shown in subsequent figures was the highest level measured by any one of the eight traverse microphones. Therefore, a directivity change that moved the peak noise to a different microphone would not appear as a noise reduction even though the noise at a specific microphone location had been reduced.

The open-loop phase sweep using 2P and 3P input are shown in Fig. 3 for the test condition of 0.15 advance ratio, 0.09 C_T/σ, and 3 deg rearward shaft tilt. Figure 3(a) shows the results for the 2P phase sweep with 1.4 deg amplitude. The 2P input is quite effective in reducing BVI noise at this test condition. Noise reduction was achieved at nearly all input phases, except at 60 deg where the noise was increased slightly. The results in the 270 deg phase region suggest that noise reduction in excess of 7 dB can be achieved using 2P input alone. The vibration index, defined as the root-mean-square of the five 3P hub load harmonics, was normalized to 1 for the HHC-Off case. The vibration index was also reduced in the phase region of minimum noise, particularly at 300 deg phase where it was reduced by about 20 percent. As mentioned previously, the rotor balance was not calibrated dynamically, and thus, the vibration index was not intended to be a precise measurement, but was useful as a general indication of the vibration level. Note that the 2P results shown in Fig. 3(a) are similar to those reported in Ref. 22 for an IBC test of a full-scale BO-105 rotor in the NASA Ames 40- by 80-Foot Wind Tunnel. Those results also showed a 7 dB reduction using the 2P input at a high BVI noise condition.

Results of the 3P phase sweep with 0.7 deg amplitude are shown in Fig. 3(b). The 3P amplitude was restricted to nearly one-half the 2P amplitude during the phase sweep because the control system loads were found to be more sensitive to this HHC component. The two structural components reaching operating limits during HHC operations were the pitch-link and the primary actuators. Since not all harmonics of the pitch-link loads were transferred to the actuators in the fixed-system, each of these two structural components was more sensitive to certain harmonics of HHC than to the others. For this test condition, the best noise reduction of 5.1 dB was achieved at 60 deg 3P phase. At this input phase, a significant increase in the 3P normal force caused an 80 percent increase in the vibration index from the baseline level. In fact, the vibration index was increased at all phases of 3P input.

With regards to rotor structural loads, test results reveal that HHC had negligible effects on the steady components but significant effects on the alternating components. Figure 4 shows the effects of 2P input on the half peak-to-peak values of the pitch-link load and blade flap and chord bending moments at 35 percent radius. The test conditions were identical to those of Fig. 3(a). The 2P input had moderate effects on the alternating blade bending moments and, in fact, showed beneficial effects at the phase region of 270 deg for minimum noise. However, the alternating pitch-link load was increased by a factor of 3 to 4 with 2P excitations.

An evaluation of the rms-pressure signal for identification of BVI noise is shown in Fig. 5. The baseline test condition was a high BVI noise condition at 0.17 advance ratio, 0.09 C_T/σ, and 3 deg rearward shaft tilt. Phase sweeps with 2P are shown in Fig. 5(a) and 3P in Fig. 5(b). Nominal amplitudes were 1.4 deg for the 2P and 0.7 deg for the 3P input. For the 2P case, BVI noise was reduced for all input phases, with a maximum reduction of 5.1 dB at 260 deg phase. The rms-pressure signal from the Kulite at 85 percent blade station agrees reasonably well with noise under 2P excitations. The agreement is particularly good at the phase region of minimum noise, a very encouraging fact for closed-loop operations. However, the 3P phase sweep results shown in Fig. 5(b) reveal a different trend. The 3P phase for minimum noise (3.5 dB reduction) was also the phase of a local maximum in the rms-pressure signal. A negative correlation between BVI noise and rms-pressure was also obtained with the 4P phase sweep at the phase of minimum noise. The pressure signal at 95 percent blade radius was contaminated with multiple perpendicular BVI events in the 90 deg azimuth region and thus was not useful for noise identification. Note that BVI noise was dominated by parallel BVI events.

Open-loop Amplitude Sweep. Amplitude sweeps were conducted at the optimum phase of each HHC harmonic. The results are shown in Fig. 6 for a high BVI noise condition (0.17 advance ratio, 0.09 C_T/σ, and 3 deg rearward shaft tilt). For each of the optimal input phases – 270 deg for 2P, 60 deg for 3P, and 150 deg for 4P input – the amplitudes were increased incrementally until the control loads reached 95 percent of operating limits. Among the three input harmonics, the 2P obtained the largest noise reduction simply because the control loads were least sensitive to this component. At the load limits, the 2P amplitude was close to 1.4 deg, while allowable amplitudes for both the 3P and 4P components were less than 0.7 deg. For this test condition, the 4P input was the most efficient and the 2P least efficient in terms of noise reduction level per deg of HHC. The noise levels varied quadratically with the 3P and 4P amplitudes.

The blade pitch schedules generated using the optimal phase angles shown in Fig. 6 reveal the fact that each of the three schedules has a maximum blade pitch near 135 deg azimuth, the region where the BVI-dominant vortex forms. Tiltrotors have a unique behavior with regards to the blade tip vortex formation. The high twist of tiltrotor blades create high inboard loading that in some flight conditions can result in a negative tip load. The reversal in loading in turn generates a pair of counter-rotating vortex, as shown with an analysis of the JVX rotor [23] and demonstrated with flow-visualizations of a small-scale V-22 rotor tested

in a descent flight condition [24]. Some noise reductions achieved in the current investigation were probably caused by either a mutual-interference of the vortex-pair before interacting with the blades or a weakening of the inboard vortex. Furthermore, since the 2P schedule has a minimum pitch at 45 deg azimuth, in the advancing BVI region, reduction in blade loading during interaction is the probable mechanism for noise reduction in this case. Finally, even though test results yield no information about the wake geometry, increases in blade-vortex miss distance is also a potential mechanism for noise reduction.

Effects of Test Condition. The effect of airspeed on noise reduction with HHC is shown in Fig. 7 using the 2P phase sweep data. The two test conditions shown in the figure differ only in airspeed (0.15 vs. 0.17 advance ratio), both having the same C_T/σ of 0.09 and 3 deg rearward shaft tilt. The nominal 2P amplitude was 1.4 deg for both cases. Since these test conditions had different baseline noise levels, the results are presented in terms of changes in the noise level, or Δ(BVI-SPL), from their respective baseline levels. In particular, the low speed case had a lower baseline noise than the higher speed case, 118.4 dB vs. 120.1 dB. The overall variations of noise with 2P phase are similar between the two test conditions. However, the condition with the lower baseline noise level (0.15 advance ratio) had a larger noise reduction, 7.1 dB vs. 5.1 dB. Similar results were obtained from the 3P and 4P phase sweeps at the low speed case.

An investigation of shaft tilt effects on noise reduction with HHC was conducted to determine whether the benefits of HHC and low-noise flight operations were additive. Open-loop HHC was applied at two additional shaft angles, 0 deg and 3 deg forward tilt, both at 0.15 advance ratio and 0.09 C_T/σ. Compared to the peak BVI noise condition at 3 deg rearward shaft tilt, these two test conditions represent the lower noise cases. All three test conditions with HHC are within the landing approach profiles of the XV-15 aircraft. The summary results, presented in Fig. 8, show the noise variation with shaft tilt angle both with and without HHC. The HHC data were the best noise reduction results obtained at the test conditions. In particular, optimal noise reduction results at 0 and 3 deg shaft angles were achieved with 2P input, while the large noise reduction at –3 deg shaft tilt (forward) was achieved with a 4P input. The results show that HHC is even more effective in reducing noise at a lower BVI noise condition, almost doubling the 7 dB reduction level achieved at the higher noise case. From the peak noise level, HHC application at a low-noise condition yielded a total reduction of 16.5 dB in BVI noise. These results suggest that HHC should best be used in combination with flight operations for low-noise approach to amplify its effectiveness.

Reduction in the Noise Footprint. The acoustic traverse was exercised to quantify the BVI directivity with HHC and to determine whether noise reduction was achieved over the entire acoustic footprint. Figure 9 shows the acoustic footprints for cases with and without HHC. The test condition was 0.15 advance ratio, 0.09 C_T/σ, and 3 deg forward shaft tilt; the 4P HHC amplitude was 0.7 deg. For the traverse results, the rotor was typically retrimmed after HHC application to match the baseline trim conditions. Since the rotor trim states were not affected in this case by the 4P input, no retrimming was necessary. The peak noise levels are located at the upper left corners of the traverse area for both cases, and the baseline peak (HHC-Off) is 114.0 dB. With HHC-On, the peak noise level is 102.0 dB. Therefore, HHC reduced the peak noise in the traverse area by 12.0 dB. Noise reduction level over the acoustic footprint was not uniform, varying from 4.2 dB to 13.6 dB. The largest noise reduction occurred in the high noise region of the baseline case.

For the noise reduction result shown in Fig. 9, HHC input had a moderate effect on the vibratory hub loads, a significant effect on the control system loads, and a negligible effect on rotor performance. The effects of 4P input on the measured 3P hub loads are shown in Fig. 10. The 4P input slightly reduced both the H-force and pitching moment and moderately increased the side force and normal force, and rolling moment. The alternating pitch-link load was increased by a factor of 4.5, and the harmonics of this load component are shown in Fig. 11. The 4P input caused a significant increase in the 4P component of the alternating pitch-link load, dominating increases in all other harmonics. The sixth and ninth harmonics of the pitch-link load increased moderately with HHC, while the steady and the 1P component were unaffected. Even though the control system hardware used in the tunnel installation were different from that of the XV-15 aircraft, these results imply that blade torsion dynamics could be an important consideration in the practical application of HHC for rotorcraft. The effects of 4P input on rotor power were small. The equivalent rotor power, a measure of power at constant propulsive force, was increased by 1 percent. This increase includes changes in both rotor shaft power and rotor drag. Because these approach flight conditions were at low shaft power, increases of this magnitude were not a concern.

Effects of Trim Perturbations on Noise Reduction. The effects of changing test conditions and trim parameters on the noise reduction results of Fig. 9 were evaluated. For this investigation, the acoustic traverse

was parked at the upstream end of the traverse area to capture the peak noise levels. The same 4P input (0.7 deg amplitude) was turned on and off while the shaft angle, advance ratio, rotor thrust, longitudinal and lateral flapping were varied independently. Shaft angle and flapping perturbations were ±1 deg, advance ratio was varied by ±5 percent, and rotor thrust was perturbed from –10 to +5 percent in 5 percent increments. The results are shown in Fig. 12. The HHC-Off baseline noise level was sensitive to shaft tilt, airspeed, rotor thrust, and longitudinal flapping and less sensitive to lateral flapping. The results with HHC showed that noise reductions remained robust with these perturbations, achieving more than 9 dB reduction in most cases. Even for the worst case with a perturbation in longitudinal flapping, the noise reduction was nearly 7 dB.

Closed-Loop Results. Closed-loop noise control was tested with different combinations of feedback signals and HHC input harmonics. Microphone feedback yielded results similar to the open-loop results. As with the open-loop cases, the noise controller was limited by control loads. Figure 13 shows noise reduction achieved with the controller using blade pressure feedback and only 2P input. The values of Q, R, and r, defined in Eqs. 2 and 3, were 1, 0.001×I, and 0.975, respectively, and I is the 2×2 identity matrix. The baseline test condition was a high noise condition (0.15 advance ratio, 0.09 C_T/σ, and 3 deg rearward shaft tilt). The rotor was retrimmed after the controller had reached a steady-state value. The peak noise levels occurred slightly to the lower left of the traverse center in both cases. The peak-to-peak reduction is 5.3 dB, 1.6 dB less than achieved with the open-loop 2P traverse (not shown). The small degradation in noise reduction with the controller suggests that the signal processing technique used for blade pressure feedback needs additional refinement.

Control of Rotor Vibratory Hub Loads

The vibration controller was tested at two forward flight conditions to evaluate the capability of multi-harmonic input to reduce rotor 3P hub loads on the XV-15 rotor. In both cases, T-matrices were identified off-line using open-loop data. The weightings for the hub load harmonics, Q, were inversely proportional to the HHC-Off values; zero weighting was assigned to the input harmonics; and r was 0.99. Figure 14 shows that the controller achieves simultaneous 3P hub loads reduction at both test conditions. The controller reduced the vibration indices by 34 percent at the lower speed and 52 percent at the higher speed. For the lower speed, the side force, normal force, and rolling moment were reduced by roughly half, while the H-force and pitching moment were reduced only slightly. For the higher speed, all hub load components except for the normal force were reduced by more than half. The increases in control system loads, reaching the operating limits, precluded the HHC authority necessary for further reduction. The root-mean-square values of HHC input for both cases were close to 0.9 deg (0.91 deg for μ of 0.125 and 0.87 deg for μ of 0.17).

Control of Rotor Trim

The automatic trim controller was evaluated at three airspeeds, and the results are presented in Table 3. In the table, the initial trim represent the trim condition achieved manually with the primary control system. The objective of the controller was to reach the target trim, and the steady-state trim are the values actually achieved by the controller. Since the controller used the dynamic control system to drive the swashplate, the system had a limited control authority. For most of the conditions shown in Table 3, the controller used the T-matrix identified off-line for that particular test condition. The values of Q, R, and r were I, 0.001×I, and 0.95, respectively, and I is the 3×3 identity matrix. To test for the controller robustness, the T-matrix identified for hover was used in two conditions in forward flight, identified with a * next to the values of the advance ratio μ. For all cases tested, the controller converged smoothly with no overshoots to the target trim values. The steady-state errors were small, less than 0.2 percent for thrust and less than 0.1 deg for flapping.

Concluding Remarks

Higher harmonic control was applied to a full-scale, isolated three-bladed XV-15 rotor in the NASA Ames 80- by 120-Foot Wind Tunnel to independently control blade-vortex interaction noise, rotor vibratory hub loads, and rotor trim. The higher harmonic blade pitch 2P–4P was generated using swashplate excitation. The radiated blade-vortex interaction (BVI) noise was measured on a plane beneath the rotor with eight microphones mounted on an acoustic traverse. Specific findings from the BVI noise reduction results are:

1. HHC was very effective in reducing BVI noise on the XV-15 rotor, achieving up to 12 dB in noise reduction.
2. The noise controller using blade pressure feedback successfully reduced BVI noise.
3. HHC was more effective for noise reduction at the lower BVI noise conditions.
4. BVI noise reduction with HHC was robust to perturbations in rotor trim and test condition.
5. The level of BVI noise reduction varied quadratically with HHC 3P and 4P amplitudes. The 4P input was the most efficient in terms of reduction level per input degree.

6. BVI noise reduction with HHC was limited by increases in control loads.
7. HHC effects on blade bending moments and rotor performance were small.
8. BVI noise reduction with HHC either increased or decreased 3P hub loads depending on the harmonic of HHC.

The vibration controller demonstrated HHC potential to reduce 3P vibratory hub loads on the XV-15 rotor in helicopter mode; increases in control load limited larger reduction. The automatic trim controller was robust and consistently tracked the target thrust and blade flapping at the conditions tested.

Acknowledgements

The results in this paper were obtained from the XV-15 Noise Reduction Test funded by the Short Haul Civil Tiltrotor (SH(CT)) Program.

The authors would like to thank Wayne Johnson, Alan Wadcock, John Madden, Doug Lillie, and the entire Wind Tunnel Operation Team led by Robert Fong, for their dedication and support throughout the entire test program.

References

1. "Civil Tiltrotor Mission and Application, Phase II: The Commercial Passenger Market," NASA CR 177576, Feb 1991.
2. Nguyen, K. and Chopra, I., "Application of Higher Harmonic Control to Hingeless Rotor Systems," *Vertica*, Vol. 14 (4), 1990.
3. Schmitz, F. and Yu, Y, "Helicopter Impulsive Noise: Theoretical and Experimental Status," *Journal of Sound and Vibration*, Vol. 109 (3), 1986.
4. Johnson, W. *Helicopter Theory*. Princeton University Press, 1980.
5. Prieur, J. and Splettstoesser, W., "ERATO – an ONERA-DLR Cooperative Programme on Aeroacoustic Rotor Optimisation," Paper No. B6, Twenty-fifth European Rotorcraft Forum, Rome, Italy, Sep 14-16, 1999.
6. Conner, D., Marcolini, M., Decker, W., Cline, J., Edwards, B., Nicks, C., Klein, P., "XV-15 Tiltrotor Low Noise Approach Operations," American Helicopter Society 55th Annual Forum Proceedings, Montreal, Canada, May 25-27, 1999.
7. Brooks, T. and Booth, E., "The Effects of Higher Harmonic Control on Blade-Vortex Interaction Noise and Vibration," *Journal of the American Helicopter Society*, Vol. 35 (3), Jul 1993.
8. Splettstoesser, W., Schultz, K., Kube, R., Brooks, T., Booth, E., Niesl, G., and Streby, O., "A Higher Harmonic Control Test in the DNW to Reduce Impulsive BVI Noise," Journal of the American Helicopter Society, Vol. 39 (4), Oct 1994.
9. Splettstoesser, W., Kube, R., Wagner, W., Seelhorst, U., Boutier, A., Micheli, F., Mercker, E., Pengel, K., "Key Results from a Higher Harmonic Control Aeroacoustic Rotor Test (HART) in the German-Dutch Wind Tunnel," Journal of the American Helicopter Society, Vol. 42 (1), Jan 1997.
10. Polychroniadis, M., "Generalized Higher Harmonic Control – Ten Years of Aerospatiale Experience," Paper No. III.7.2, Sixteenth European Rotorcraft Forum, Glasgow, England, Sep 18-20, 1990.
11. Wood, E., Powers, R., Cline, J., and Hammond, C., "On Developing and Flight Testing a Higher Harmonic Control System," Journal of the American Helicopter Society, Vol. 30 (1), Jan 1985.
12. Miao, W., Kottapalli, S., and Frye, H., "Flight Demonstration of Higher Harmonic Control on the S-76 Rotor," American Helicopter Society 42nd Annual Forum Proceedings, Washington, D.C., Jun 2-4, 1986.
13. Polychroniadis, M., Achache, M., "Higher Harmonic Control: Flight Test on a SA 349 Research Gazelle," American Helicopter Society 42nd Annual Forum Proceedings, Washington, D.C., Jun 2-4, 1986.
14. Hammond, C., "Wind Tunnel Results Showing Rotor Vibratory Loads Reduction Using Higher Harmonic Blade Pitch," Journal of the American Helicopter Society, Vol. 28 (1), Jan 1983.
15. Shaw, J., Albion, N., Hanker, E., and Teal, R., "Higher Harmonic Control: Wind Tunnel Demonstration of Fully Effective Vibratory Hub Force Suppression," Journal of the American Helicopter Society, Vol. 34 (1), Jan 1989.
16. Nixon, M., Kvaternik, R., and Settle, B., "Tiltrotor Vibration Reduction through Higher Harmonic Control," American Helicopter Society 53rd Annual Forum Proceedings, Virginia Beach, VA, Apr 29-May 1, 1997.
17. Swanson, S., Jacklin, S., Blaas, A., Niesl, G., and Kube, R., "Acoustic Results from a Full-Scale Wind Tunnel Test Evaluating Individual Blade Control," American Helicopter Society 51st Annual Forum Proceedings, Ft. Worth, TX, May 9-11, 1995.
18. Splettstoesser, W., Schultz, K., van der Wall, B., Buchholz, H., Gembler, W., and Niesl, G., "The Effect of Individual Blade Pitch Control on BVI Noise – Comparison of Flight Test and Simulation Results," Paper No. AC07, Twenty-fourth European Rotorcraft Forum, Marseille, France, Sept 15-17, 1998.
19. Marcolini, M., Booth, E., Tadghighi, H., Hassan, H., Smith, C., and Becker, L., "Control of BVI Noise Using an Active Trailing Edge Flap," American Helicopter Society 1995 Vertical Lift Aircraft Design Conference, San Francisco, CA, Jan 18-20, 1995.
20. Kitaplioglu, C., Betzina, M., and Johnson, W., "Blade-Vortex Interaction Noise of an Isolated Full-Scale XV-15 Tilt-Rotor," American Helicopter Society 56th Annual Forum Proceedings, Virginia Beach, VA, May 2-4, 2000.
21. Kitaplioglu, C., McCluer, M., and Acree, C., "Comparison of XV-15 Full-Scale Wind Tunnel and In-Flight Blade-Vortex Interaction Noise," American Helicopter Society 53rd Annual Forum Proceedings, Virginia Beach, VA, Apr 29-May 1, 1997.
22. Jacklin, S., Nguyen, K., and Blass, A., and Richter, P., "Full-Scale Wind Tunnel Test of a Helicopter Individual Blade Control (IBC) System," Proceedings of the 50th American Helicopter Society Annual Forum, Washington, D.C., May 1994.
23. Burley, C., Marcolini, M., Brooks, T., Brand, A., and Conner, D., "Tiltrotor Aeroacoustic Code (TRAC) Predic-

tions and Comparison with Measurements," American Helicopter Society 52nd Annual Forum Proceedings, Washington, D.C., Jun 4-6, 1996.
24. Yamauchi, G, Burley, C., Mercker, E., Pengel, K., and JanakiRam, R., "Flows Measurements of an Isolated Model Tilt Rotor," American Helicopter Society 55th Annual Forum Proceedings, Montreal, Canada, May 25-27, 1999.

Table 1. General Rotor Properties

Number of blades	3
Rotor radius, ft	12.5
Blade chord (constant), in	14.0
Rotor solidity, thrust-weighted, σ	0.089
Blade twist (nonlinear), deg	40.9
Hub precone, deg	1.5
Blade Lock number	3.83
Nominal rotor rpm	589
Hover tip Mach number	0.691

Table 2. HHC Test Conditions

			Primary objectives				
			BVI Noise				
μ	CT/σ (nominal)	α, deg	Open-Loop	Closed-loop		Vibration	Trim
				Mic	Press		
0.170	.090	3	X		X		
0.150	.090	3	X	X	X		
0.150	.090	0	X		X		
0.150	.090	–3	X		X		
0.000	.077	0					X
0.125	.090	–2				X	X
0.170	.090	–5				X	X

Table 3. Test Results for the Automatic Trim Controller

		Initial Trim (nominal)			Target Trim			Steady-state Trim		
μ	α deg	Thrust lbs	Long Flap deg	Lat Flap deg	Thrust lbs	Long Flap deg	Lat Flap deg	Thrust lbs	Long Flap deg	Lat Flap deg
0	0	4700	0.7	0.7	4300	0.0	0.0	4309	–.02	–.04
0	0	4700	0.7	–.7	4300	0.0	0.0	4295	.06	.07
0	0	4700	0.0	0.0	5000	0.5	–.5	4989	.48	–.41
0.125	–2	5600	0.7	0.7	6000	0.0	0.0	6011	–.03	.00
0.125	–2	5600	0.7	–.7	5200	0.0	0.0	5207	–.03	–.01
0.125*	–2	5600	0.5	–.5	5200	0.0	0.0	5208	–.01	–.01
0.17	–5	5600	0.7	0.7	6000	0.0	0.0	6006	.02	–.01
0.17	–5	5600	0.7	–.7	5200	0.0	0.0	5199	–.01	.03
0.17*	–5	5600	0.5	–.5	5200	0.0	0.0	5196	–.03	.03

* Trim controller used T-matrix identified in hover.

Fig. 1. Isolated XV-15 Rotor on the Rotor Test Apparatus in the 80- by 120-Foot Wind Tunnel.

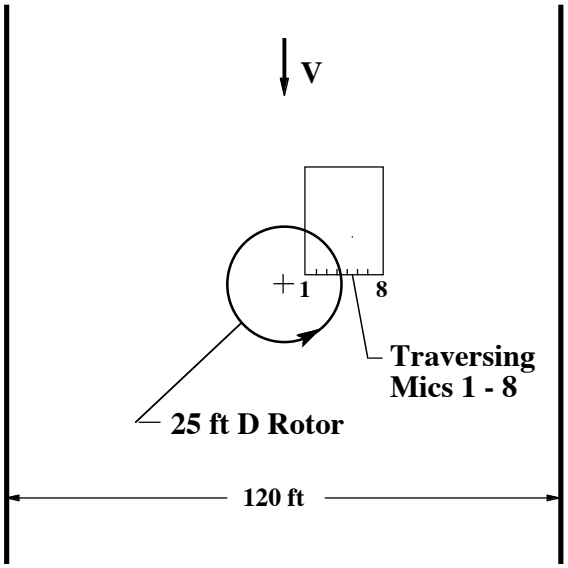

Fig. 2. Microphone locations for the XV-15 Test in the 80- by 120-Foot test section.

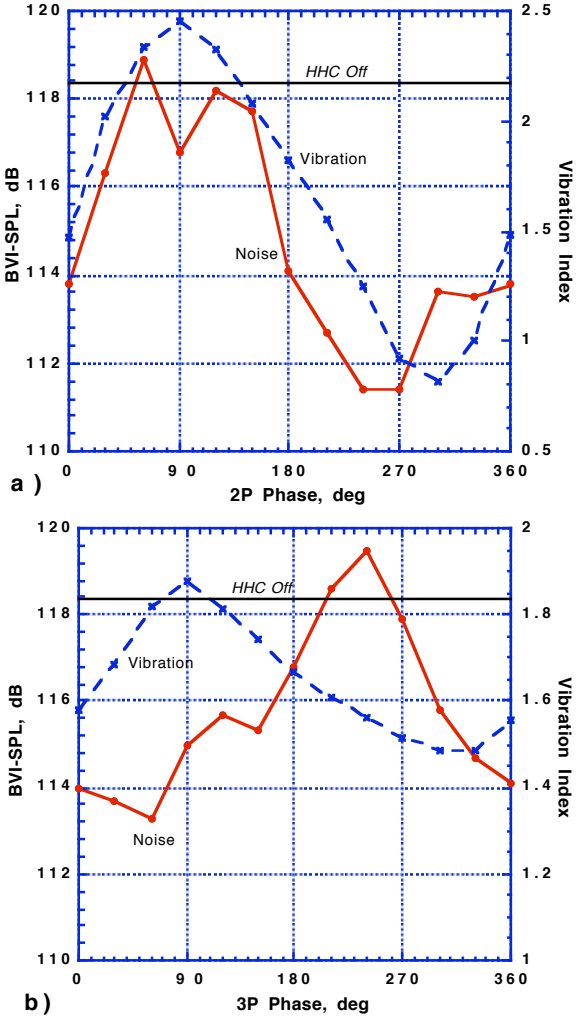

Fig. 3. Variation of BVI noise and 3P hub loads with HHC phase, (a) 2P sweep, 1.4 deg amplitude, (b) 3P sweep, 0.7 deg amplitude. $\mu = 0.15$, $C_T/\sigma = 0.09$, $\alpha = 3$ deg aft.

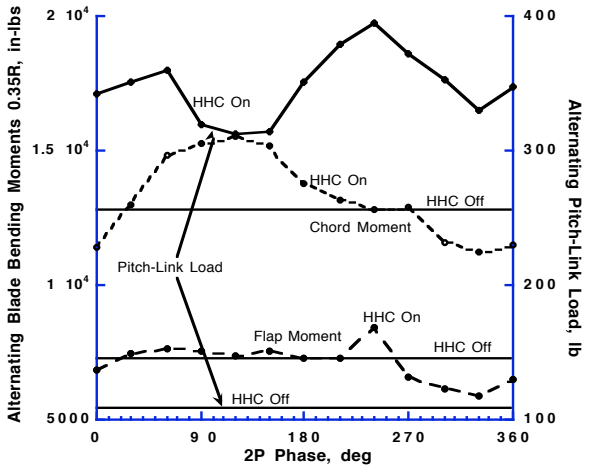

Fig. 4. Variation of alternating blade bending moments and pitch-link load with 2P HHC phase, 1.4 deg amplitude. $\mu = 0.15$, $C_T/\sigma = 0.09$, $\alpha = 3$ deg aft.

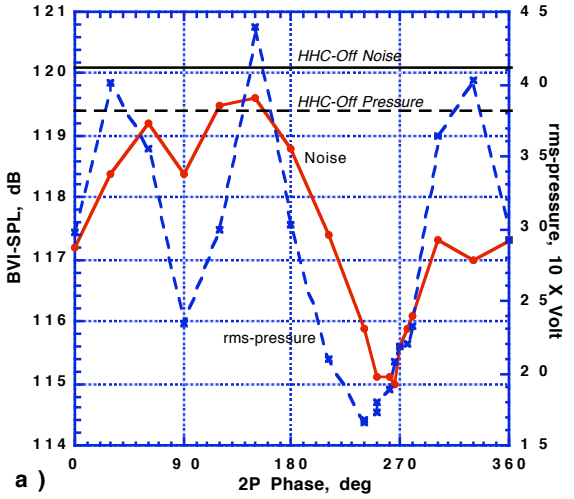

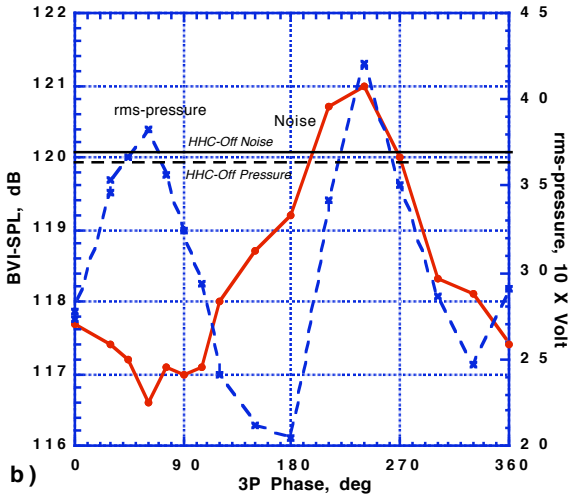

Fig. 5. Variation of BVI noise and rms-pressure signal at 0.85R with HHC phase, (a) 2P HHC, 1.4 deg amplitude, (b) 3P HHC, 0.7 deg amplitude. $\mu = 0.17$, $C_T/\sigma = 0.09$, $\alpha = 3$ deg aft.

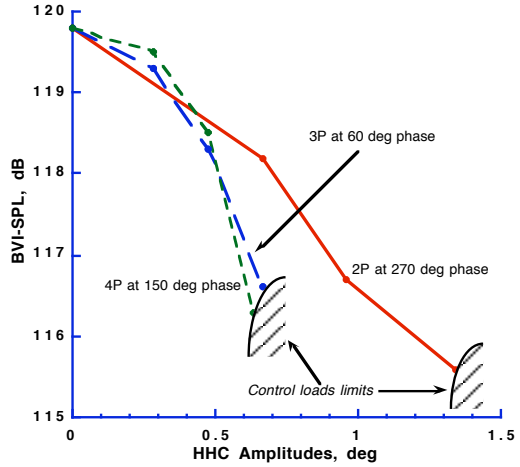

Fig. 6. Variation of BVI noise with HHC amplitude at phases of best noise reduction. $\mu = 0.17$, $C_T/\sigma = 0.09$, $\alpha = 3$ deg aft.

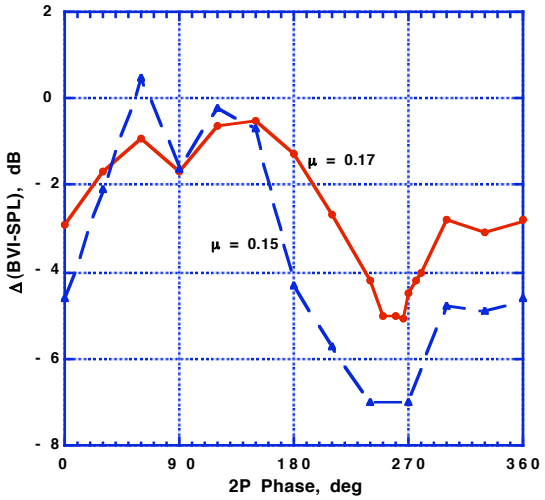

Fig. 7. Variation of BVI noise with 2P HHC phase, 1.4 deg amplitude, at two advance ratios. $C_T/\sigma = 0.09$, $\alpha = 3$ deg aft.

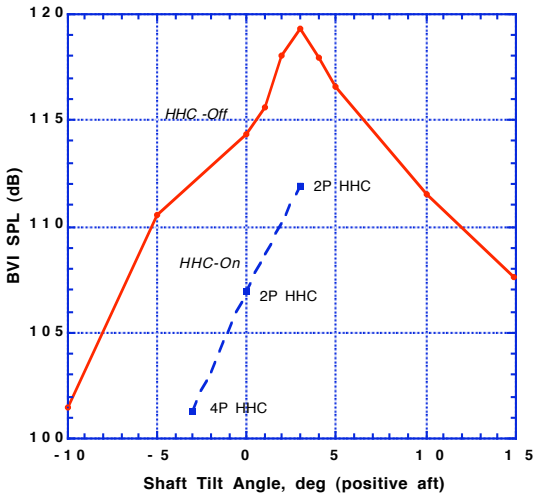

Fig. 8. BVI noise reduction with HHC at different rotor shaft angles. $\mu = 0.15$, $C_T/\sigma = 0.09$.

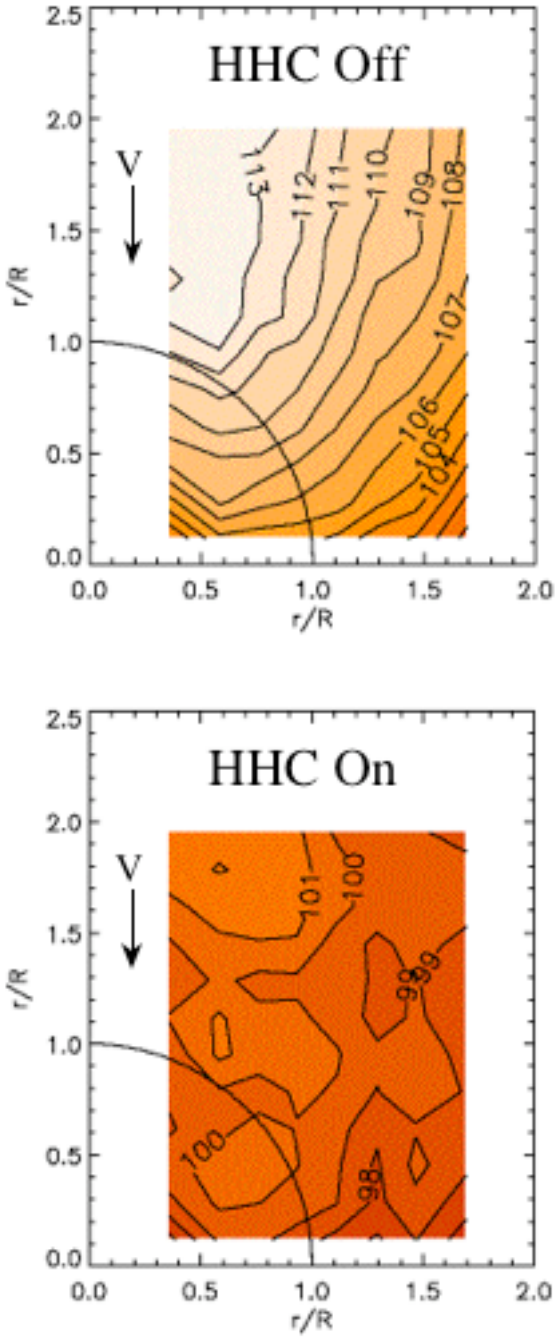

Fig. 9. Noise reduction with 4P HHC over BVI-SPL contour. $\mu = 0.15$, $C_T/\sigma = 0.09$, $\alpha = 3$ deg forward.

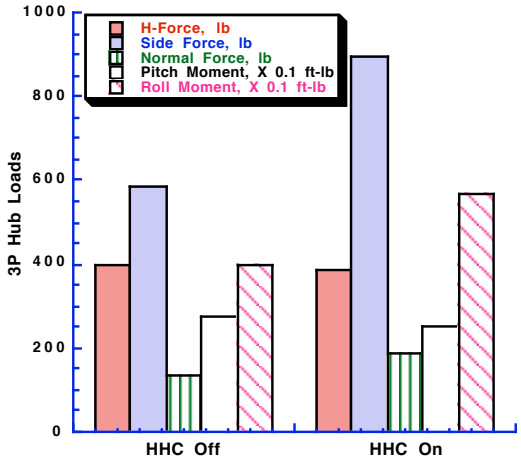

Fig. 10. Effect of 4P HHC for noise reduction on 3P hub loads. $\mu = 0.15$, $C_T/\sigma = 0.09$, $\alpha = 3$ deg.forward.

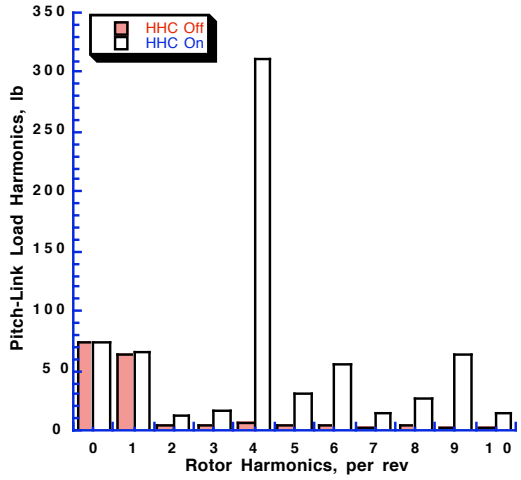

Fig. 11. Effect of 4P HHC for noise reduction on harmonics of pitch-link load. $\mu = 0.15$, $C_T/\sigma = 0.09$, $\alpha = 3$ deg forward.

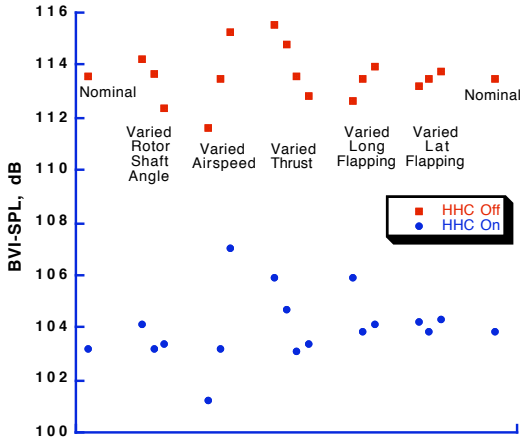

Fig. 12. Effects of trim and flight condition perturbations (increasing left to right) on BVI noise reduction with HHC. Baseline condition: $\mu = 0.15$, $C_T/\sigma = 0.09$, $\alpha = 3$ deg forward.

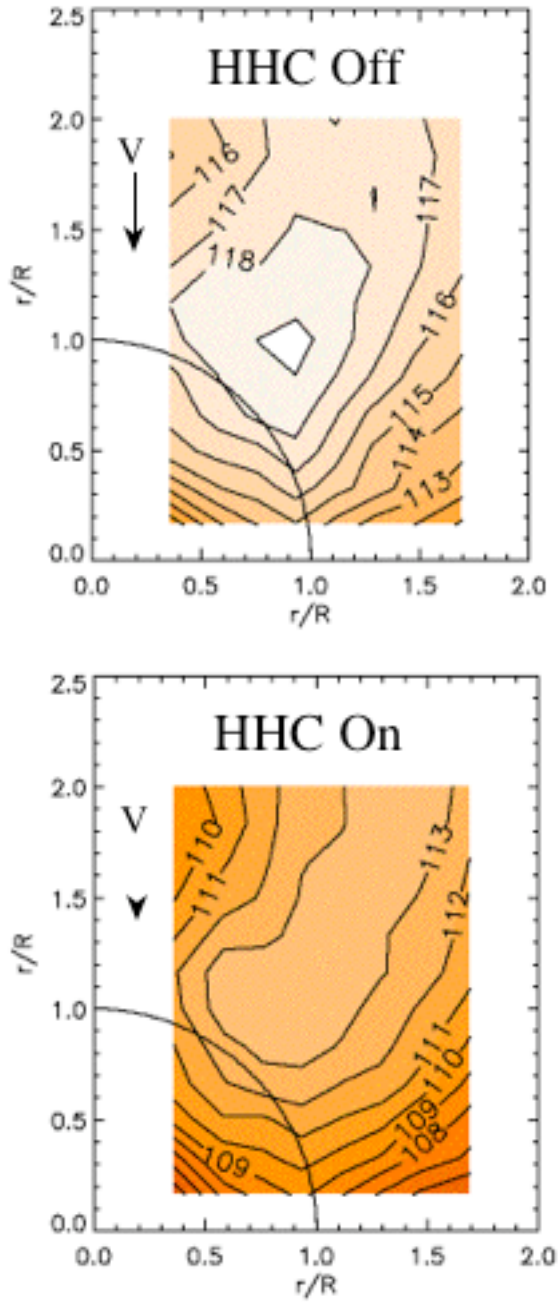

Fig. 13. Noise reduction using noise controller with blade pressure feedback over BVI-SPL contour. $\mu = 0.15$, $C_T/\sigma = 0.09$, $\alpha = 3$ deg aft.

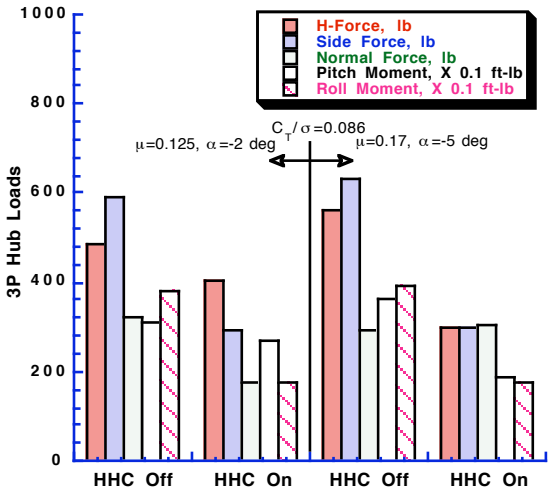

Fig. 14. Reduction in 3P hub loads with the vibration controller at two forward flight conditions.